



HAL
open science

Uncertainty Quantification of Eruption Source Parameters Estimated From Tephra Fall Deposits

R. Constantinescu, J. T. White, C. B. Connor, A. Hopulele-Gligor, S. Charbonnier, J. -C. Thouret, J. M. Lindsay, D. Bertin

► To cite this version:

R. Constantinescu, J. T. White, C. B. Connor, A. Hopulele-Gligor, S. Charbonnier, et al.. Uncertainty Quantification of Eruption Source Parameters Estimated From Tephra Fall Deposits. *Geophysical Research Letters*, 2022, 49, 10.1029/2021GL097425 . insu-03708903

HAL Id: insu-03708903

<https://insu.hal.science/insu-03708903>

Submitted on 29 Jun 2022

HAL is a multi-disciplinary open access archive for the deposit and dissemination of scientific research documents, whether they are published or not. The documents may come from teaching and research institutions in France or abroad, or from public or private research centers.

L'archive ouverte pluridisciplinaire **HAL**, est destinée au dépôt et à la diffusion de documents scientifiques de niveau recherche, publiés ou non, émanant des établissements d'enseignement et de recherche français ou étrangers, des laboratoires publics ou privés.



Distributed under a Creative Commons Attribution 4.0 International License

Geophysical Research Letters®



RESEARCH LETTER

10.1029/2021GL097425

Uncertainty Quantification of Eruption Source Parameters Estimated From Tephra Fall Deposits

Key Points:

- Characterising volcanic eruptions based on incompletely preserved and sampled tephra deposits leads to uncertainty in classification
- We couple a tephra forward model to two inversion techniques to quantify eruption parameter uncertainty
- Results show uncertainty quantification is crucial for sparsely sampled deposits because range in eruption parameters can be substantial

R. Constantinescu¹ , J. T. White² , C. B. Connor¹, A. Hopulele-Gligor³, S. Charbonnier¹, J.-C. Thouret⁴, J. M. Lindsay⁵, and D. Bertin⁵

¹School of Geosciences, University of South Florida, Tampa, FL, USA, ²INTERA Inc., Boulder, CO, USA, ³Independent Software Engineer, Cluj-Napoca, Romania, ⁴Université Clermont Auvergne, Laboratoire Magmas et Volcans, CNRS, OPGC et IRD, Aubière, France, ⁵School of Environment, University of Auckland, Auckland, New Zealand

Supporting Information:

Supporting Information may be found in the online version of this article.

Correspondence to:

R. Constantinescu,
robert.constantinescu00@gmail.com

Citation:

Constantinescu, R., White, J. T., Connor, C. B., Hopulele-Gligor, A., Charbonnier, S., Thouret, J.-C., et al. (2022). Uncertainty quantification of eruption source parameters estimated from tephra fall deposits. *Geophysical Research Letters*, 49, e2021GL097425. <https://doi.org/10.1029/2021GL097425>

Received 13 DEC 2021
Accepted 10 MAR 2022

Author Contributions:

Conceptualization: R. Constantinescu, J. T. White, C. B. Connor
Data curation: R. Constantinescu, J. T. White, A. Hopulele-Gligor
Formal analysis: R. Constantinescu, J. T. White, C. B. Connor, S. Charbonnier
Methodology: R. Constantinescu, J. T. White, C. B. Connor
Resources: S. Charbonnier, J.-C. Thouret, J. M. Lindsay, D. Bertin
Software: R. Constantinescu, J. T. White, C. B. Connor, A. Hopulele-Gligor
Writing – original draft: R. Constantinescu, J. T. White, C. B. Connor

© 2022. The Authors.

This is an open access article under the terms of the [Creative Commons Attribution License](https://creativecommons.org/licenses/by/4.0/), which permits use, distribution and reproduction in any medium, provided the original work is properly cited.

Abstract Uncertainty quantification (UQ) in eruption source parameters, like tephra volume, plume height, and umbrella cloud radius, is a challenge for volcano scientists because tephra deposits are often sparsely sampled due to burial, erosion, and related factors. We find that UQ is improved by coupling an advection-diffusion model with two Bayesian inversion approaches: (a) a robust but computationally expensive Generalized Likelihood Uncertainty Estimation algorithm, and (b) a more approximate but inexpensive parameter estimation algorithm combined with first-order, second-moment uncertainty estimation. We apply the two inversion methods to one sparsely sampled tephra fall unit from the 2070 BP El Misti (Peru) eruption and obtain: Tephra mass $0.78\text{--}1.4 \times 10^{11}$ kg; umbrella cloud radius 4.5–16.5 km, and plume height 8–35 km (95% confidence intervals). These broad ranges demonstrate the significance of UQ for eruption classification based on mapped deposits, which has implications for hazard management.

Plain Language Summary Volcanologists use ashfall deposits to estimate the magnitudes and intensities of past or unobserved eruptions. Different processes can affect the ash deposits during and after the eruption (e.g., burial, remobilisation, and erosion) resulting in sparse sampling of the deposit and uncertainty in the deposit thickness where it is sampled. Uncertain data results in uncertain estimates of erupted volume, plume height, and umbrella cloud dimensions, which are essential parameters used to estimate future volcanic hazards. Here we present two methods to quantify the uncertainty in these parameter estimates from deposit data. As a case study, we estimate eruption parameters for a sparsely sampled ashfall deposit from the 2070 BP eruption of El Misti, Peru. We find that for this sampled unit the mass of the erupted tephra was $0.78\text{--}1.4 \times 10^{11}$ kg, umbrella cloud radius was 4.5–16.5 km, and plume height was 8–35 km. These ranges are 95% confidence intervals, giving a much better idea of the eruption magnitude and intensity than that is achieved from point estimates, such as reporting the erupted mass as a single value.

1. Introduction

Tephra deposit thickness and its variation in mappable deposits is a source of data used to quantify the dynamics of past volcanic eruptions (e.g., Fierstein & Nathenson, 1992; Newhall & Self, 1982; Pyle, 1989; Pyle, 2015). Eruption source parameters (ESPs) used to quantify the eruption magnitude and intensity include tephra mass/volume, plume height, umbrella cloud radius, total grain size variation, and mass discharge rate. ESPs are derived from deposit data using empirical, analytical, and numerical models, particularly for past eruptions (e.g., Bonadonna & Costa, 2012; Bonadonna et al., 2005; Carey & Sparks, 1986; Rossi et al., 2019). The relationship of ESPs to eruption deposit thickness is a nonlinear and underdetermined/ill-posed inverse problem (White et al., 2017). This inverse problem is data poor. Many combinations of ESP values reproduce the observed deposit thinning as a function of distance and direction from the volcano, leading to uncertainty in the estimated ESPs. Uncertainty quantification (UQ) is as important as point estimates of ESPs when classifying eruptions based on geologic data. The range of uncertainty provides an evaluation of our confidence in estimated ESPs, for the purposes of assessing eruption hazards.

Random variability in tephra deposits is one source of uncertainty in estimating ESPs. Variations in the thicknesses of tephra fallout in stratigraphic sections can be related to factors like slope, orographic conditions, remobilization, and observational uncertainty (Buckland et al., 2020; Engwell et al., 2013). Natural variability includes the distribution of observable tephra sections, impacted by preservation. For example, distal and thin stratigraphic

Writing – review & editing: R. Constantinescu, J. T. White, C. B. Connor, A. Hopulele-Gligor, S. Charbonnier, J.-C. Thouret, J. M. Lindsay, D. Bertin

sections tend to erode faster than near-vent deposits, which are buried by more recent deposits. Consequently, some of the largest eruptions in Earth's history are either misclassified or missing from stratigraphic records (e.g., Kiyosugi et al., 2015). Deposit data contribute to aleatoric uncertainty, meaning there is random variation in tephra thickness with distance from the volcano that is not associated with ESPs. Unfortunately, this aleatoric variation influences the estimate of ESPs. Methods of deposit volume estimation based on interpolation of isolines of equal deposit thickness from tephra sections underestimate aleatoric uncertainty and misestimate volume by up to 50% (Biass et al., 2019; Engwell et al., 2013; Klawonn et al., 2014; Prival et al., 2019; Sulpizio, 2005).

A second source of uncertainty stems from how models, statistical or numerical, are used to estimate ESPs from tephra data. Statistical models that are used to estimate volume include exponential, power-law, and Weibull, with model parameters estimated from interpolated isopach data (e.g., Bonadonna & Costa, 2012; Fierstein & Nathenson, 1992; Pyle, 1989). These models may or may not describe the data adequately, especially when they are used to extrapolate trends beyond the limits of available tephra sections (Bonadonna & Costa, 2012). Statistical model choice is a source of epistemic uncertainty. Numerical models based on the advection-diffusion equation (ADE) are sensitive to all ESPs. Deposit thickness is estimated at each tephra section locality based on a set of ESPs and forward modeling with the ADE (e.g., Bonadonna et al., 2005; Connor et al., 2001; Costa et al., 2006; Hurst & Turner, 1999; Macedonio et al., 2005; Pfeiffer et al., 2005). Epistemic uncertainty stems from how well the forward model, which uses uncertain ESPs as inputs, captures the physical processes of tephra dispersion during specific eruptions. Numerical models simplify the processes that control the sedimentation (e.g., simplified volcanic plume geometry and wind field) and these simplifications potentially impact the estimation of ESPs (e.g., Mannen et al., 2020; Yang et al., 2021). For example, models that do not account for the umbrella cloud geometry for volcanic explosivity index (VEI) ≥ 4 eruptions yield biased results (Constantinescu et al., 2021). As aleatoric and epistemic uncertainties are always present, reconstruction of the dynamics of explosive eruptions through modeling and ESP estimation is challenging (Figure 1).

We couple an ADE model with two Bayesian inversion and UQ approaches: (a) a more approximate, assumption-laden, but computationally inexpensive Bayesian parameter estimation algorithm combined with first-order, second-moment UQ based on the Gaussian-Levenburg-Marquardt algorithm-first-order, second-moment (GLM-FOSM) (White et al., 2017), and (b) the Generalized Likelihood Uncertainty Estimation (GLUE) algorithm (Beven & Binley, 1992). As a test case, we invert deposit thickness of a sparsely sampled tephra fall unit from the 2070 BP El Misti (Peru) eruption (e.g., Cobeñas et al., 2012; Harpel et al., 2011). We estimate total erupted mass, umbrella cloud radius and height, diffusion coefficient, mean grain size distribution and wind field, and the uncertainty associated with these parameters. We consider the trade-off between more rigorous and more approximate probabilistic inversion methods to estimate ESPs (i.e., GLUE vs. GLM-FOSM). This analysis demonstrates that ESPs are inadequately characterized by single value estimates. Instead, ESPs should be reported using confidence intervals, resulting in better understanding of eruption hazards based on previous volcanic activity (Figure 1) (e.g., Bonasia et al., 2010; Primerano et al., 2021). The two inversion approaches, which we compare and contrast, each offer a method of estimating these confidence intervals.

2. Data and Prior Information

The 2070 BP eruption of El Misti (Peru) was a Plinian (VEI 4) event that produced extensive pumice fall and flow deposits (Supplementary Note 1 in Supporting Information S1; Charbonnier et al., 2020; Cobeñas et al., 2012, 2014; Harpel et al., 2011; Thouret et al., 2001). We sample the lower-most lapilli-rich tephra fall unit from this complex eruption and measure its deposit thickness at 30 localities (Supplementary Note 1; Figure S1 in Supporting Information S1). This unit is identified as the upper part of Layer 1 of Cobeñas et al. (2012) and as Bed 2 of Harpel et al. (2011), and is one of the most easily recognized units across the medial facies SW of the volcano. The measured localities are mostly located between ~6 and 26 km from the volcano because elsewhere the deposit is eroded or disturbed by urban development.

We invert the thickness of this tephra unit and estimate seven ESPs (Table 1). Deposit thickness is the most commonly used source of information to estimate ESPs; here we do not use grain size information. The inversions are guided by prior distributions defined by a range of realistic values for each ESP. The parameter boundaries are based on expert knowledge of the eruption (Cobeñas et al., 2012; Thouret et al., 2001) and constrained to physically plausible values (e.g., eruptive columns are <55 km high; Wilson et al., 1978).

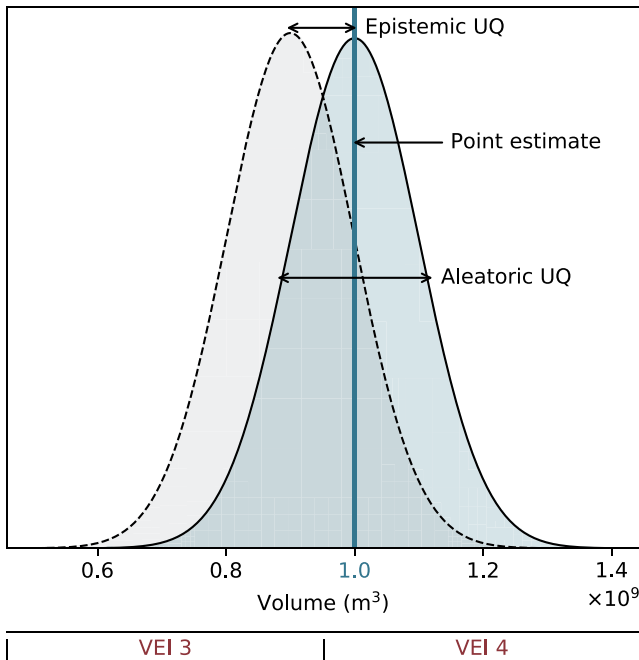


Figure 1. Schematic example of aleatoric and epistemic uncertainty quantification associated with point estimates of eruption volume and the effect on eruption classification using the volcanic explosivity index scale.

3. Forward Model

Tephra sedimentation is estimated with the forward model developed by Constantinescu et al. (2021) and based on the Tephra2 algorithm (Bonadonna et al., 2005; Connor and Connor, 2006). The model assumes an umbrella cloud inserted into the atmosphere as a circular or elliptical disk, discretized in grid cells, at a neutral buoyancy height above the vent (e.g., Bonadonna & Phillips, 2003; Bursik et al., 1992; Costa et al., 2013; Mastin et al., 2014; Sparks et al., 1997). The disk does not account for the dynamics of a laterally spreading plume. The umbrella region is well mixed (i.e., umbrella cloud diameter is reached when umbrella spreading velocity is smaller than wind velocity, e.g., Bursik et al., 1992; Carey & Sparks, 1986). Tephra falls from the base of the cloud and is advected by wind.

The total mass of tephra accumulated at a ground location ($M(x, y)$) is:

$$M(x, y) = \sum_{c_j=1}^{c_j^{max}} \sum_{\phi_{min}}^{\phi_{max}} M_{c_j, \phi}^0 f_{c_j, \phi}(x, y) \quad (1)$$

where the mass contribution ($M_{c_j, \phi}^0$) of particles of each ϕ size is released from each source location in the disk (c_j). $f_{c_j, \phi}(x, y)$ calculates ground mass accumulation at coordinates (x, y) for each particle size released from each disk cell and accounts for particle diffusion through a turbulent atmosphere and advection by a wind field. In practice, the total mass of particles is binned in 100 bins from -6ϕ to $+6\phi$ and is uniformly divided among 8.5×10^3 disk grid cells. The position and accumulation of particles on the ground depends on (a) the mass and distribution of each particle size, (b) particle position in the disk relative to the vent and the number of disk cells, (c) the height of the base of the disk, (d) the uniform horizontal diffusion of the atmosphere, and (e) the wind speed and direction (assumed to be constant in the model). Unlike other models (e.g., Poulidis et al., 2021), we assume no vertical wind or vertical diffusion and particle accumulation occurs on a flat topography.

4. Inversion Models

Inversion is used to estimate ESPs from the forward model and deposit data, given ESPs prior distributions. In GLUE analysis (Beven & Binley, 1992), a large prior ensemble, which represents the plausible range of ESPs, is filtered based on “behavioral” characteristics related to reproducing the observed tephra deposit data. A rigorous

Table 1
Estimated Eruption Source Parameters and the Search Domain Boundaries for Generalized Likelihood Uncertainty Estimation Method (Uniform Prior Distribution) and the GLM-FOSM Method (Gaussian Prior Distribution With Prior Mean)

Parameter	Prior information				Posterior estimates			
	GLUE		GLM-FOSM		GLUE		GLM-FOSM	
	Lower bound	Upper bound	Prior mean	Prior σ	Posterior mean	Posterior σ	Posterior mean	Posterior σ
Erupted mass ($\text{kg} \times 10^{11}$)	0.1	5.0	1.0	1.2	0.9	0.2	1.0	0.1
Umbrella height ($\text{m.a.v.} \times 10^3$)	10	30	25	5	20	6	25	4.8
Umbrella radius ($\text{m} \times 10^3$)	5	25	11	5	10.5	3	11	3.2
TGSD (ϕ)	-2	2	-1.9	1	0.9	0.7	1.1	0.6
Diffusion ($\text{m}^2 \text{s}^{-1} \times 10^3$)	0.3	3	1.5	0.7	2.0	0.6	1.5	0.5
Wind speed (m s^{-1})	0.5	20	5	4.8	1.7	0.7	1.2	0.5
Wind direction (0 from N)	160	260	220	25	218	4.3	218	5.8

Note. The posterior means and standard deviations are at $\pm 2\sigma$ for 95% confidence interval. *m.a.v.* = meters above vent.

rejection-sampling method is used to estimate the uncertainty in ESPs, based on the assumptions that complex natural systems such as volcanic eruptions cannot be represented by one set of ESPs but rather that multiple combinations of ESPs. Each prior realization of ESP values in the prior ensemble is evaluated with the model to produce a simulated tephra deposit. Each simulated tephra thickness is compared against the observed deposit thickness using a summary statistic criterion (e.g., residual sum of squares [RSS]) established a priori. The prior ESP realizations associated with simulation outputs that acceptably reproduce the tephra thickness observations are termed “behavioral” and retained (Beven & Binley, 1992, 2014; Beven & Freer, 2001). Collectively, a large number of behavioral ESP realizations are found by Monte Carlo sampling.

As an alternative ESP estimation approach, the forward model is coupled to the GLM-FOSM algorithm through the *pestpp-glm* software tool (White et al., 2017, 2020). This approach pairs gradient-based minimum-error-variance parameter estimation with prior and posterior Bayes-linear parameter uncertainty estimation, which assumes the prior and posterior parameter distribution are (log) Gaussian. The GLM-FOSM approach is computationally very efficient but requires additional assumptions compared to the GLUE analysis. We used the same parameterization for the GLM-FOSM as for the GLUE analysis, however, because of its inherent assumptions, the GLM-FOSM analysis employs a multivariate Gaussian prior parameter distribution in place of the uniform prior distribution used in GLUE (Table 1).

5. Results

5.1. GLUE Analysis and UQ

A total of 1×10^6 model runs were completed for the GLUE analysis, corresponding to 1×10^6 prior ESP realizations, each representing a set of plausible ESP values. We retain 96 model realisations that best match the observed thicknesses (an acceptance ratio of $RSS \leq 1.25 \times \text{best_RSS}$). The uncertainty in ESPs is summarized in Figure 2 and Table 1.

The conditioning provided by the tephra thickness is evaluated by how much uncertainty is reduced in the posterior distribution compared with the prior distribution. The total eruption mass in the prior ranges from 0.1 to 5×10^{11} kg (VEI 3 to 4). The total erupted mass is one of the most conditioned parameters; the uncertainty range is significantly reduced in the posterior estimate to $0.5\text{--}1.4 \times 10^{11}$ kg. When compared to the uniform prior distribution, inversion reduces the uncertainty in the eruption mass estimate by more than 80%. The umbrella cloud radius was estimated between 4.5 and 16.5 km, a 40% uncertainty reduction compared to its prior.

The umbrella cloud height (i.e., height at the base of the cloud) is a highly uncertain parameter and we assign a uniform prior search domain between 10 and 30 km above vent. The inversion estimates a mean of 20 km a.s.l. with a 95% confidence interval between 8 and 32 km, indicating a poorly constrained parameter. This is a natural result in ill-posed inverse problems; the deposit data do not have sufficient unique information to condition this ESP. The umbrella cloud height and diffusion coefficient show only minor differences between the prior and the posterior estimates indicating two dependent parameters. The uncertainty in diffusion coefficient is reduced by $\sim 15\%$. The posterior mean of the total grain size distribution is 0.9ϕ , with an uncertainty range between -0.5ϕ and 2.3ϕ . Wind direction is related to the distribution of the samples and easily inferred, but the wind speed during past eruptions is challenging to estimate. Given the assumptions of the model (i.e., average wind field across the simulated grid area), the mean wind speed was estimated between 0.5 and 3 m s^{-1} with 95% confidence.

5.2. GLM-FOSM Analysis and UQ

The GLM-FOSM analysis used 99 model runs and generally agrees with GLUE analysis (Figure 2; Table 1). The GLM-FOSM best estimate for the erupted mass is $\sim 1 \times 10^{11}$ kg with a 95% confidence interval between 0.78 and 1.2×10^{11} kg; the uncertainty in posterior was reduced by $\sim 90\%$. The umbrella cloud radius estimate is ~ 11 km with the uncertainty decreased by $\sim 30\%$. No significant uncertainty reduction was achieved in the posterior umbrella cloud height estimate ($\sim 3\%$). The posterior diffusion coefficient estimate is slightly improved when compared with the prior ($\sim 17\%$), given the relationship with the umbrella cloud radius and height (i.e., high diffusion is no longer required to account for wider spread of tephra). Considerable uncertainty reduction was obtained for the wind direction and speed; the uncertainty in the posterior estimate was reduced by more than 80%. The mean posterior grain size distribution was estimated at 1.12ϕ (-0.1ϕ – 2.3ϕ , 95% confidence).

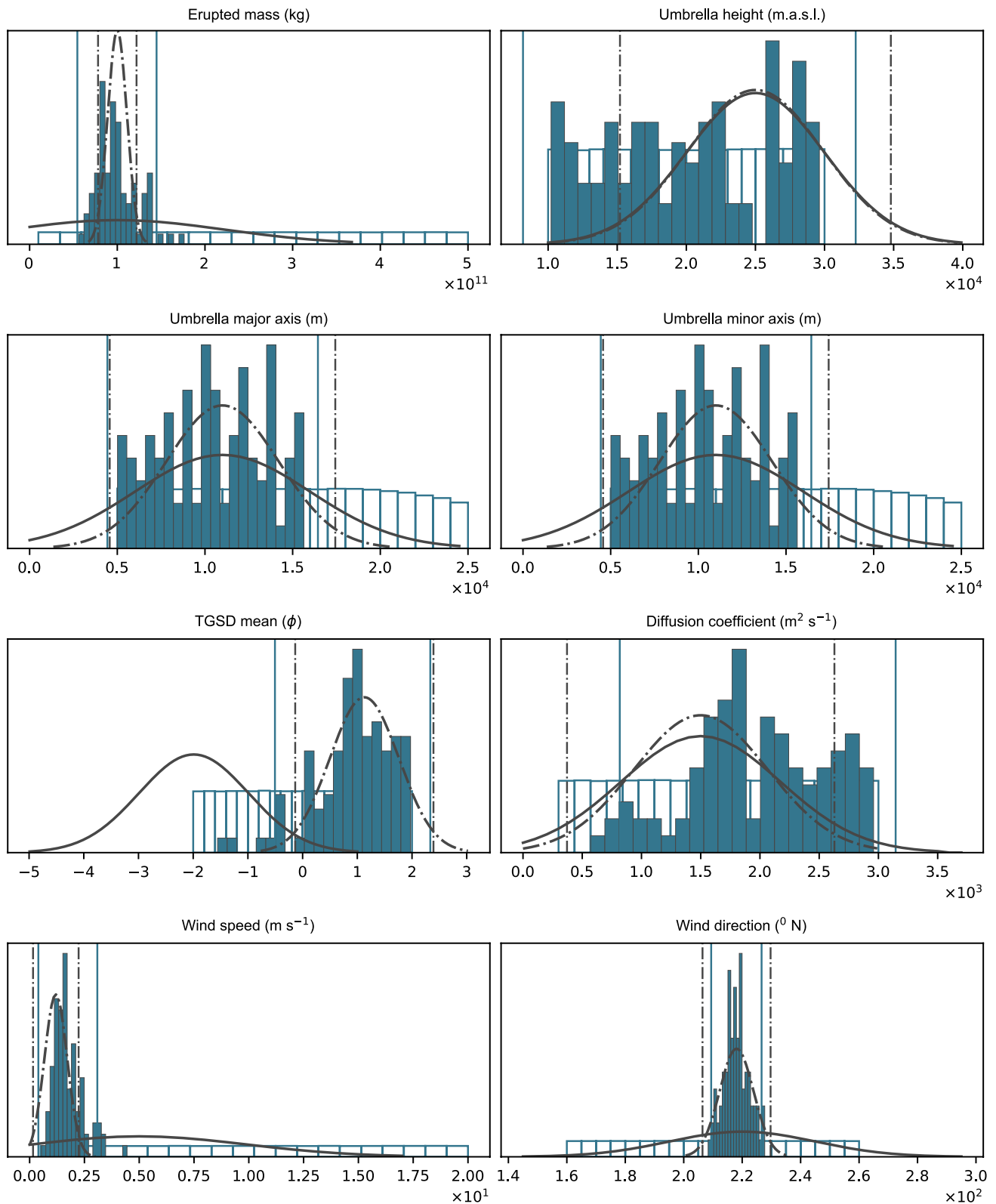


Figure 2. Generalized Likelihood Uncertainty Estimation analysis—*hollow histograms* show the uniform prior ensemble and *solid blue histograms* show the posterior estimates. GLM-FOSM analysis—the *solid line Gaussian* show the prior ensemble and the *dashed line Gaussian* the posterior estimate. The vertical lines represent the 95% confidence interval (*solid blue* for GLUE; *dashed gray* for GLM-FOSM).

6. Discussion and Final Remarks

There is a varying posterior uncertainty in the estimated ESPs when using deposit thickness data to infer the dynamics of the eruption because this information is not sufficient to condition all uncertain ESPs. In this case study, the selected tephra layer has highly variable thickness throughout the medial facies (~10–35 cm; Supplementary Note 1 in Supporting Information S1). We attribute this variability to the roughness of topography (i.e., deep and steep valleys separated by relatively flatter interfluves) combined with postdepositional processes (e.g., Buckland et al., 2020; Engwell et al., 2013; Green et al., 2016). While the tephra deposit was buried and compacted by thick pyroclastic flow deposits in the valleys (Charbonnier et al., 2020; Thouret et al., 2001), the exposed material on the interfluves was subjected to intense erosion (Cobeñas et al., 2012). Owing to the climatic conditions, deposits in the distal facies (>26 km from the vent) are poorly preserved and a vast area of the medial facies has been covered by the city of Arequipa. The availability of outcrops for this tephra layer leads to a sparsely sampled deposit with the majority of thickness measurements taken in the near medial facies. Few distal points were available to constrain the deposit. These factors contribute to aleatoric uncertainty for ESPs (Connor et al., 2019). The GLUE and GLM-FOSM inversion methods explain roughly equal amounts of variation in deposit thickness, as reflected by the coefficient of determination (r^2) (Figures 3a–3d). Both reveal that only some ESPs are well constrained due to aleatoric uncertainty.

The regression analysis coefficients of determination, 0.68 and 0.69, respectively, indicate that approximately two thirds of the variation in mapped deposit thickness is explained by best-fit models, regardless of the inversion method. This result agrees with Engwell et al. (2013) who suggested that random variation in deposit thicknesses may be on order of 30%.

Erupted mass is the best constrained parameter by both inversion methods. The erupted mass is well constrained because of the linear dependency between ground mass tephra accumulation and the total erupted mass in the forward model (e.g., Magill et al., 2015; White et al., 2017). This model efficiency is reflected in the reduction of uncertainty in the posterior compared to the prior using GLUE and GLM-FOSM methods. Both inversion methods rely on the definition of a prior parameter distribution that effectively defines the plausible search domain, which is subjective. The GLUE method gives more flexibility in the prior. In this case, we used a uniform random prior distribution. The ensemble inversion results shift the posterior mean substantially compared to the prior, and narrows the 95% confidence interval on total erupted mass. The GLM-FOSM inversion method requires a Gaussian prior distribution. The posterior is shifted only slightly. Experimentation shows that the GLM-FOSM method does not achieve good model fits if the prior varies substantially from the posterior distribution. In other words, the GLUE method is computationally much more expensive, but yields a robust estimate of the total eruption mass ESP. In contrast, unless the prior mean of the GLM-FOSM approach is in the appropriate region of attraction, the total eruption mass may be less well estimated, and RMSE will be larger, indicating a poorer model fit.

The umbrella cloud radius is relatively well informed given the dependency between the position of particles accumulated on the ground and their release position in the disk relative to the vent location. Tephra sedimentation occurs directly under the leading edge of the umbrella cloud (e.g., Carey & Sparks, 1986; Sparks et al., 1997); sedimentation over this limit is attributed to atmospheric diffusion and wind advection. We look at the deposit to define a search domain for the umbrella cloud radius between 10 and 30 km (i.e., assuming sedimentation either occurred from a small cloud in high wind, or from a larger cloud and lower wind). An umbrella cloud radius of ~11 km seems to provide the best fit. As with total erupted mass, the GLUE inversion method starts with a broader prior and finds a posterior comparable with GLM-FOSM.

As sedimentation is controlled by particle fall time and atmospheric properties (e.g., Bonadonna & Costa, 2013; Connor et al., 2019; Volentik et al., 2010), the umbrella cloud height, the mean grain size distribution, and diffusion coefficient are associated with larger posterior uncertainty. We noticed in simulations that pairs of “*high plumes—small umbrella clouds*” associated with “*high diffusion—low wind speed*” can replicate the deposit equally well—a critical nonuniqueness (e.g., Bonasia et al., 2010; White et al., 2017). In other words, the same deposit thickness can be modeled at a given distance from the volcano with coarse grain sizes released from a high umbrella cloud, or fine grain sizes released from a low umbrella cloud. Some of these parameter trade-offs are physically implausible and are addressed with a prior distribution constrained by plausible boundaries. Assuming a Plinian event, here we use the vent altitude (~5,800 m a.s.l.) and the tropopause level at this latitude (~16,000 m a.s.l.) to define the prior for umbrella height between 10 and 30 km above vent. Although most

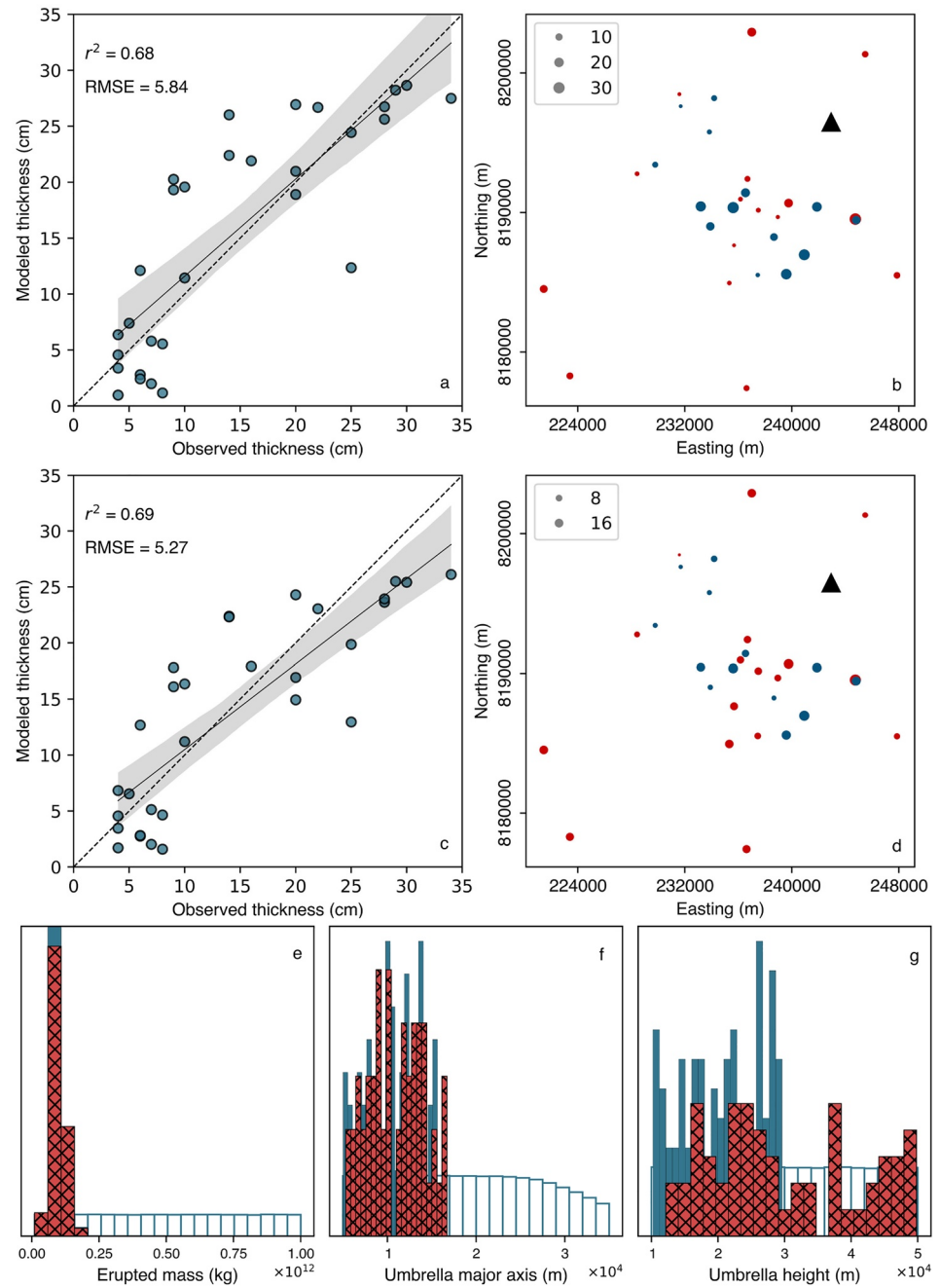


Figure 3. Correlation between observed and modeled tephra thickness from the lowest RSS Generalized Likelihood Uncertainty Estimation (GLUE) (a) and GLM-FOSM (c). The negative (*blue*) and positive (*red*) residual thicknesses downwind from the vent (triangle) for GLUE (b) and GLM-FOSM (d). The diameter of the points indicates the magnitude of the residual thicknesses. Histograms show the estimates for erupted mass (e), umbrella cloud radius (f), and umbrella cloud height (g) using a wider parameter search domain. The *hollow blue histograms* show the prior distribution, the *solid blue histograms* show the posterior estimates from the original search domain (Table 1; Figure 2), and the *hatched red histograms* show the posterior estimates from the larger parameter search domain.

umbrella clouds form at tropopause level where the atmospheric properties change, higher levels were observed for other Plinian events (e.g., Mt. St. Helens, 10–20 km (Sparks et al., 1986); Pinatubo, >20 km (Koyaguchi & Tokuno, 1993; Suzuki & Koyaguchi, 2009)). Reducing uncertainty in umbrella height is dependent on model assumptions and number of measurements. Given the simplified wind profile assumed by the model, few measurements, and no grain size data, no constraints are made on particle fall time, resulting in higher uncertainties in

umbrella cloud height estimates (8–32 km). Previous studies showed that using grain size information in tephra sedimentation models constrains particle fall time and therefore plume height (e.g., Bonasia et al., 2010; Costa et al., 2016; Mele et al., 2020; Volentik et al., 2010). Here we invert only deposit thickness and this results in poorer constraints of umbrella height. For similar reasons, the posterior mean grain size was associated with high uncertainty. From expert knowledge and assuming an efficient fragmentation associated with Plinian eruptions (e.g., Dufek et al., 2012), we define a prior mean grain size between -2ϕ and $+2\phi$ with a posterior estimate peaking around $\sim 1\phi$ a value comparable with those reported by Cobeniñas et al. (2012).

One of the goals of tephra sedimentation models is to lower the diffusion coefficient to more physically plausible values, that is, reduce the use of this ESP as a compensatory parameter. Using a disk source in sedimentation models decreases the need for unrealistically high diffusion coefficients (Constantinescu et al., 2021). We constrain the search domain for this parameter between 300 and 3,000 $\text{m}^2 \text{s}^{-1}$ and observe that most model realizations tend to form a peak around 1,700 $\text{m}^2 \text{s}^{-1}$. We also notice that increasing wind speed to decrease diffusion leads to thinner deposits as finer particles are likely blown away. These two parameters are not mutually exclusive and both contribute to the sedimentation patterns observed in the field. The uncertainty in wind speed and direction is reduced significantly, although this is an average value, given models' assumptions.

The sensitivity of estimated ESP values to the choice ESP prior distribution was further investigated by running additional 1×10^6 GLUE model realizations using wider prior distributions for the erupted mass (10^{10} – 10^{12} kg), umbrella cloud radius (5–35 km), and height (10–50 km). The best estimated parameters, total eruption mass, and umbrella cloud radius converge on the same posterior estimates as using an inflated prior distribution (Figures 3e and 3f). Based on the expected value of total eruption mass and umbrella cloud radius (Constantinescu et al., 2021), the eruption that produced this tephra unit was most likely VEI 4, in agreement with previous estimates (Harpel et al., 2011; Cobeniñas et al., 2012; Supplementary Note 1 in Supporting Information S1).

While both inversion methods we presented have their merit, the GLM-FOSM analysis is much more efficient at UQ and provides a probabilistic estimate of ESPs within minutes running on a regular desktop computer. GLUE is able to provide a more robust estimate of the posterior ESPs, with the cost of longer computation times. Posterior ESPs can be refined for contemporary eruptions by providing prior parameter distributions constrained by observations of plume heights or umbrella cloud radii. Using data sets from the proximal and distal facies along with grain size information may reduce the uncertainty in ESP estimates regardless of the inversion method. Ultimately, both methods presented here provide insight into how well ESPs are constrained by a given tephra thickness data set, an improvement over point estimates of ESPs (Figure 1). Understanding the magnitude of this uncertainty will improve our assessment of volcanic hazards.

Conflict of Interest

The authors declare no conflicts of interest relevant to this study.

Data Availability Statement

The computer models developed and used in this study, along with the field data, are available at <https://zenodo.org/record/6079900>.

References

- Beven, K., & Binley, A. (1992). The future of distributed models: Model calibration and uncertainty prediction. *Hydrological Processes*, 6(3), 279–298. <https://doi.org/10.1002/hyp.3360060305>
- Beven, K., & Binley, A. (2014). GLUE: 20 years on. *Hydrological Processes*, 28(24), 5897–5918. <https://doi.org/10.1002/hyp.10082>
- Beven, K., & Freer, J. (2001). Equifinality, data assimilation, and uncertainty estimation in mechanistic modelling of complex environmental systems using the GLUE methodology. *Journal of Hydrology*, 249(1), 11–29. [https://doi.org/10.1016/S0022-1694\(01\)00421-8](https://doi.org/10.1016/S0022-1694(01)00421-8)
- Biass, S., Bonadonna, C., & Houghton, B. F. (2019). A step-by-step evaluation of empirical methods to quantify eruption source parameters from tephra-fall deposits. *Journal of Applied Volcanology*, 8(1), 1. <https://doi.org/10.1186/s13617-018-0081-1>
- Bonadonna, C., Connor, C. B., Houghton, B. F., Connor, L. J., Byrne, M., Laing, A., & Hincks, T. K. (2005). Probabilistic modeling of tephra dispersal: Hazard assessment of a multiphase rhyolitic eruption at Tarawera, New Zealand. *Journal of Geophysical Research: Solid Earth*, 110(B3), B03203. <https://doi.org/10.1029/2003jb002896>
- Bonadonna, C., & Costa, A. (2012). Estimating the volume of tephra deposits: A new simple strategy. *Geology*, 40(5), 415–418. <https://doi.org/10.1130/g32769.1>

Acknowledgments

This research was partially supported by a grant from the U.S. National Science Foundation (NSF 1841928). JCT acknowledges support from the Institute of Research for the Development and I-SITE CAP-2025 (French government) challenge 4 “Social and economic impacts from volcanic activity.” We wish to thank our editor (Christian Huber) and our reviewers (Samantha Engwell and one anonymous reviewer) for the suggestions and comments that improved this manuscript.

- Bonadonna, C., & Costa, A. (2013). Modeling tephra sedimentation from volcanic plumes. In R. M. C. Lopes, S. A. Fagents, & T. K. P. Gregg (Eds.), *Modeling volcanic processes: The physics and mathematics of volcanism* (pp. 173–202). Cambridge University Press.
- Bonadonna, C., & Phillips, J. C. (2003). Sedimentation from strong volcanic plumes. *Journal of Geophysical Research: Solid Earth*, 108(B7), 2340. <https://doi.org/10.1029/2002jb002034>
- Bonasia, R., Macedonio, G., Costa, A., Mele, D., & Sulpizio, R. (2010). Numerical inversion and analysis of tephra fallout deposits from the 472AD sub-Plinian eruption at Vesuvius (Italy) through a new best-fit procedure. *Journal of Volcanology and Geothermal Research*, 189(3), 238–246. <https://doi.org/10.1016/j.jvolgeores.2009.11.009>
- Buckland, H. M., Cashman, K. V., Engwell, S. L., & Rust, A. C. (2020). Sources of uncertainty in the Mazama isopachs and the implications for interpreting distal tephra deposits from large magnitude eruptions. *Bulletin of Volcanology*, 82(3), 23. <https://doi.org/10.1007/s00445-020-1362-1>
- Bursik, M. I., Carey, S. N., & Sparks, R. S. J. (1992). A gravity current model for the May 18, 1980 Mount St. Helens plume. *Geophysical Research Letters*, 19(16), 1663–1666. <https://doi.org/10.1029/92gl01639>
- Carey, S., & Sparks, R. S. J. (1986). Quantitative models of the fallout and dispersal of tephra from volcanic eruption columns. *Bulletin of Volcanology*, 48(2), 109–125. <https://doi.org/10.1007/bf01046546>
- Charbonnier, S. J., Thouret, J.-C., Gueugneau, V., & Constantinescu, R. (2020). New insights into the 2070calyrBP pyroclastic currents at El Misti volcano (Peru) from field investigations, satellite imagery and probabilistic modeling. *Frontiers of Earth Science*, 8(398). Original Research. <https://doi.org/10.3389/feart.2020.557788>
- Cobeñas, G., Thouret, J.-C., Bonadonna, C., & Boivin, P. (2012). The c.2030yr BP Plinian eruption of El Misti volcano, Peru: Eruption dynamics and hazard implications. *Journal of Volcanology and Geothermal Research*, 241–242, 105–120. <https://doi.org/10.1016/j.jvolgeores.2012.06.006>
- Cobeñas, G., Thouret, J.-C., Bonadonna, C., & Boivin, P. (2014). “Reply to comment on Cobeñas, G., Thouret, J.-C., Bonadonna, C., & Boivin, P. The c.2030yr BP Plinian eruption of El Misti volcano, Peru: Eruption dynamics and hazard implications, *Journal of Volcanology and Geothermal Research* 241–242, 105–120.” by Harpel et al., *JVGR* 2013. *Journal of Volcanology and Geothermal Research*, 275, 103–113. <https://doi.org/10.1016/j.jvolgeores.2014.02.014>
- Connor, C. B., Connor, L. J., Bonadonna, C., Luhr, J., Savov, I., & Navarro-Ochoa, C. (2019). Modelling tephra thickness and particle size distribution of the 1913 eruption of volcán de Colima, Mexico. In N. Varley, C. B. Connor, & J.-C. Komorowski (Eds.), *Volcán de Colima: Portrait of a persistently hazardous volcano* (pp. 81–110). Springer Berlin Heidelberg. https://doi.org/10.1007/978-3-642-25911-1_3
- Connor, C. B., Hill, B. E., Winfrey, B., Franklin, N. M., & Femina, P. (2001). Estimation of volcanic hazards from tephra fallout. *Natural Hazards Review*, 2(1), 33–42. [https://doi.org/10.1061/\(asce\)1527-6988\(2001\)2:1\(33\)](https://doi.org/10.1061/(asce)1527-6988(2001)2:1(33))
- Connor, L. J., & Connor, C. B. (2006). Inversion is the key to dispersion: Understanding eruption dynamics by inverting tephra fallout. In H. Mader, S. C. Coles, C. B. Connor, & L. J. Connor (Eds.), *Statistics in volcanology* (Vol. 231–242). Geological Society.
- Constantinescu, R., Hopulele-Gligor, A., Connor, C. B., Bonadonna, C., Connor, L. J., Lindsay, J. M., et al. (2021). The radius of the umbrella cloud helps characterize large explosive volcanic eruptions. *Communications Earth & Environment*, 2(1), 3. <https://doi.org/10.1038/s43247-020-00078-3>
- Costa, A., Folch, A., & Macedonio, G. (2013). Density-driven transport in the umbrella region of volcanic clouds: Implications for tephra dispersion models. *Geophysical Research Letters*, 40(18), 4823–4827. <https://doi.org/10.1002/grl.50942>
- Costa, A., Macedonio, G., & Folch, A. (2006). A three-dimensional Eulerian model for transport and deposition of volcanic ashes. *Earth and Planetary Science Letters*, 241(3), 634–647. <https://doi.org/10.1016/j.epsl.2005.11.019>
- Costa, A., Pioli, L., & Bonadonna, C. (2016). Assessing tephra total grain-size distribution: Insights from field data analysis. *Earth and Planetary Science Letters*, 443, 90–107. <https://doi.org/10.1016/j.epsl.2016.02.040>
- Dufek, J., Manga, M., & Patel, A. (2012). Granular disruption during explosive volcanic eruptions. *Nature Geoscience*, 5(8), 561–564. <https://doi.org/10.1038/ngeo1524>
- Engwell, S. L., Sparks, R. S. J., & Aspinall, W. P. (2013). Quantifying uncertainties in the measurement of tephra fall thickness. *Journal of Applied Volcanology*, 2(1), 5. <https://doi.org/10.1186/2191-5040-2-5>
- Fierstein, J., & Nathenson, M. (1992). Another look at the calculation of fallout tephra volumes. *Bulletin of Volcanology*, 54(2), 156–167. <https://doi.org/10.1007/bf00278005>
- Green, R. M., Bebbington, M. S., Jones, G., Cronin, S. J., & Turner, M. B. (2016). Estimation of tephra volumes from sparse and incompletely observed deposit thicknesses. *Bulletin of Volcanology*, 78(4), 25. <https://doi.org/10.1007/s00445-016-1016-5>
- Harpel, C. J., de Silva, S., & Salas, G. (2011). *The 2 ka eruption of Misti volcano, southern Peru—the most recent plinian eruption of Arequipa’s iconic volcano*. (Vol. 484). Geological Society of America.
- Hurst, A. W., & Turner, R. (1999). Performance of the program ASHFALL for forecasting ashfall during the 1995 and 1996 eruptions of Ruapehu volcano. *New Zealand Journal of Geology and Geophysics*, 42(4), 615–622. <https://doi.org/10.1080/00288306.1999.9514865>
- Kiyosugi, K., Connor, C., Sparks, R. S. J., Crosweiler, H. S., Brown, S. K., Siebert, L., et al. (2015). How many explosive eruptions are missing from the geologic record? Analysis of the quaternary record of large magnitude explosive eruptions in Japan. *Journal of Applied Volcanology*, 4(1), 17. <https://doi.org/10.1186/s13617-015-0035-9>
- Klawonn, M., Houghton, B. F., Swanson, D. A., Fagents, S. A., Wessel, P., & Wolfe, C. J. (2014). Constraining explosive volcanism: Subjective choices during estimates of eruption magnitude. *Bulletin of Volcanology*, 76(2), 793. <https://doi.org/10.1007/s00445-013-0793-3>
- Koyaguchi, T., & Tokuno, M. (1993). Origin of the giant eruption cloud of Pinatubo, June 15, 1991. *Journal of Volcanology and Geothermal Research*, 55(1), 85–96. [https://doi.org/10.1016/0377-0273\(93\)90091-5](https://doi.org/10.1016/0377-0273(93)90091-5)
- Macedonio, G., Costa, A., & Longo, A. (2005). A computer model for volcanic ash fallout and assessment of subsequent hazard. *Computers & Geosciences*, 31(7), 837–845. <https://doi.org/10.1016/j.cageo.2005.01.013>
- Magill, C., Mannen, K., Connor, L., Bonadonna, C., & Connor, C. (2015). Simulating a multi-phase tephra fall event: Inversion modelling for the 1707 Hoei eruption of Mount Fuji, Japan. *Bulletin of Volcanology*, 77(9), 81. <https://doi.org/10.1007/s00445-015-0967-2>
- Mannen, K., Hasenaka, T., Higuchi, A., Kiyosugi, K., & Miyabuchi, Y. (2020). Simulations of tephra fall deposits from a bending eruption plume and the optimum model for particle release. *Journal of Geophysical Research: Solid Earth*, 125(6), e2019JB018902. <https://doi.org/10.1029/2019JB018902>
- Mastin, L. G., Van Eaton, A. R., & Lowenstern, J. B. (2014). Modeling ash fall distribution from a Yellowstone supereruption. *Geochemistry, Geophysics, Geosystems*, 15(8), 3459–3475. <https://doi.org/10.1002/2014gc005469>
- Mele, D., Costa, A., Dellino, P., Sulpizio, R., Dioguardi, F., Isaia, R., & Macedonio, G. (2020). Total grain size distribution of components of fallout deposits and implications for magma fragmentation mechanisms: Examples from campi flegrei caldera (Italy). *Bulletin of Volcanology*, 82(4), 31. <https://doi.org/10.1007/s00445-020-1368-8>

- Newhall, C. G., & Self, S. (1982). The volcanic explosivity index (VEI) an estimate of explosive magnitude for historical volcanism. *Journal of Geophysical Research*, 87(C2), 1231–1238. <https://doi.org/10.1029/jc087ic02p01231>
- Pfeiffer, T., Costa, A., & Macedonio, G. (2005). A model for the numerical simulation of tephra fall deposits. *Journal of Volcanology and Geothermal Research*, 140(4), 273–294. <https://doi.org/10.1016/j.jvolgeores.2004.09.001>
- Poulidis, A. P., Biass, S., Bagheri, G., Takemi, T., & Iguchi, M. (2021). Atmospheric vertical velocity - A crucial component in understanding proximal deposition of volcanic ash. *Earth and Planetary Science Letters*, 566, 116980. <https://doi.org/10.1016/j.epsl.2021.116980>
- Primerano, P., Giordano, G., Costa, A., de Vita, S., & Di Vito, M. A. (2021). Reconstructing fallout features and dispersal of Cretatio Tephra (Ischia Island, Italy) through field data analysis and numerical modelling: Implications for hazard assessment. *Journal of Volcanology and Geothermal Research*, 415, 107248. <https://doi.org/10.1016/j.jvolgeores.2021.107248>
- Prival, J. M., Thouret, J. C., Japura, S., Gurioli, L., Bonadonna, C., Mariño, J., & Cueva, K. (2019). New insights into eruption source parameters of the 1600 CE Huaynputina Plinian eruption, Peru. *Bulletin of Volcanology*, 82(1), 7. <https://doi.org/10.1007/s00445-019-1340-7>
- Pyle, D. M. (1989). The thickness, volume and grainsize of tephra fall deposits. *Bulletin of Volcanology*, 51(1), 1–15. <https://doi.org/10.1007/bf01086757>
- Pyle, D. M. (2015). Chapter 13 - sizes of volcanic eruptions. In H. Sigurdsson (Ed.), *The encyclopedia of volcanoes* (2nd edn., pp. 257–264). Academic Press. <https://doi.org/10.1016/b978-0-12-385938-9.00013-4>
- Rossi, E., Bonadonna, C., & Degruyter, W. (2019). A new strategy for the estimation of plume height from clast dispersal in various atmospheric and eruptive conditions. *Earth and Planetary Science Letters*, 505, 1–12. <https://doi.org/10.1016/j.epsl.2018.10.007>
- Sparks, R. S. J., Bursik, M. I., Carey, S. N., Gilbert, J., Glaze, L. S., Sigurdsson, H., & Woods, A. (1997). *Volcanic plumes*. Wiley.
- Sparks, R. S. J., Moore, J. G., & Rice, C. J. (1986). The initial giant umbrella cloud of the May 18th, 1980, explosive eruption of Mount St. Helens. *Journal of Volcanology and Geothermal Research*, 28(3), 257–274. [https://doi.org/10.1016/0377-0273\(86\)90026-0](https://doi.org/10.1016/0377-0273(86)90026-0)
- Sulpizio, R. (2005). Three empirical methods for the calculation of distal volume of tephra-fall deposits. *Journal of Volcanology and Geothermal Research*, 145(3), 315–336. <https://doi.org/10.1016/j.jvolgeores.2005.03.001>
- Suzuki, Y. J., & Koyaguchi, T. (2009). A three-dimensional numerical simulation of spreading umbrella clouds. *Journal of Geophysical Research*, 114(B3). <https://doi.org/10.1029/2007jb005369>
- Thouret, J.-C., Finizola, A., Fornari, M., Legeley-Padovani, A., Suni, J., & Frechen, M. (2001). Geology of El Misti volcano near the city of Arequipa, Peru. *GSA Bulletin*, 113(12), 1593–1610. [https://doi.org/10.1130/0016-7606\(2001\)113<1593:goemvn>2.0.co;2](https://doi.org/10.1130/0016-7606(2001)113<1593:goemvn>2.0.co;2)
- Volentik, A. C. M., Bonadonna, C., Connor, C. B., Connor, L. J., & Rosi, M. (2010). Modeling tephra dispersal in absence of wind: Insights from the climactic phase of the 2450BP Plinian eruption of Pululagua volcano (Ecuador). *Journal of Volcanology and Geothermal Research*, 193(1), 117–136. <https://doi.org/10.1016/j.jvolgeores.2010.03.011>
- White, J. T., Connor, C. B., Connor, L., & Hasenaka, T. (2017). Efficient inversion and uncertainty quantification of a tephra fallout model. *Journal of Geophysical Research: Solid Earth*, 122(1), 281–294. <https://doi.org/10.1002/2016jb013682>
- White, J. T., Hunt, R. J., Fienen, M. N., & Doherty, J. E. (2020). *Approaches to highly parameterized inversion: PEST++ version 5, a software suite for parameter estimation, uncertainty analysis, management optimization and sensitivity analysis (7-C26)*. Retrieved from <https://pubs.er.usgs.gov/publication/tm7C26>
- Wilson, L., Sparks, R. S. J., Huang, T. C., & Watkins, N. D. (1978). The control of volcanic column heights by eruption energetics and dynamics. *Journal of Geophysical Research*, 83(B4), 1829–1836. <https://doi.org/10.1029/jb083ib04p01829>
- Yang, Q., Pitman, E. B., Bursik, M., & Jenkins, S. F. (2021). Tephra deposit inversion by coupling Tephra2 with the metropolis-Hastings algorithm: Algorithm introduction and demonstration with synthetic datasets. *Journal of Applied Volcanology*, 10(1), 1. <https://doi.org/10.1186/s13617-020-00101-4>